ACS SENSORS

pubs.acs.org/acssensors

Article

Ultrasensitive and Low-Cost Paper-Based Graphene Oxide Nanobiosensor for Monitoring Water-Borne Bacterial Contamination

Stalin Karuppiah, Narayan Chandra Mishra, Wei-Chen Tsai, Wei-Ssu Liao, and Chia-Fu Chou*

Cite This: *ACS Sens.* 2021, 6, 3214−3223

Read Online

ACCESS | Metrics & More | Article Recommendations | Supporting Information

ABSTRACT: Water-borne pathogens are mostly generated due to poor sanitation, industrial effluents, and sewage sludge, leading to a significant increase in mortality rate. To prevent this, we need a simple, user-friendly, and rapid on-site detection tool of pathogens, i.e., a biosensor. As contaminated water mainly contains (80%) coliform bacteria, of which *Escherichia coli* is the major species, we have developed a screen-printed paper-based, label-free biosensor for the detection of *E. coli* in water. A nanoarchitectured graphene oxide (GO), as a fast electron-transfer flatland, was deposited on the screen-printed graphene (G) on a hydrophobic paper, followed by the immobilization of lectin Concanavalin A (ConA) as a biorecognition element for a GGO_ConA-biosensing electrode. The electrochemical characterization of GGO_ConA shows fast electron transfer with a calculated electroactive surface area of 0.16 cm^2. The biosensor performance was tested in the sludge water and beach water (real sample) as an analyte using the electrochemical impedance spectroscopy (EIS) technique. The charge-transfer resistance (R_{ct}) of GGO_ConA increases linearly with the bacterial concentration in the range of $10-10^8$ CFU mL^{-1} with an estimated limit of detection (LOD) of 10 CFU mL^{-1}, which indicates the ultrasensitivity of our biosensor, with 100 times more sensitivity than previous studies. Our reported biosensor, being cost-effective, eco-friendly, and ultrasensitive, may serve greatly as a portable monitoring kit for checking water-borne bacterial contamination.

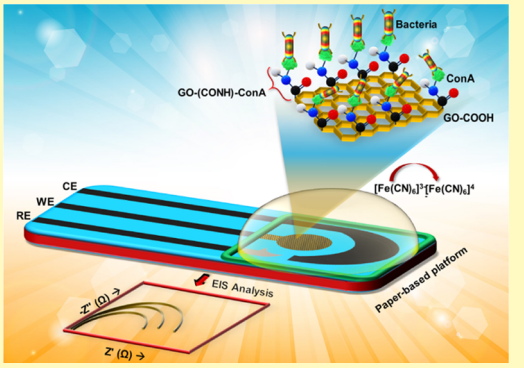

KEYWORDS: *water-borne pathogens, E. coli, paper-based biosensors, screen-printed electrode, graphene, impedimetric sensing*

Sustainable and clean water management among developing nations remains a huge challenge due to poor infrastructure, weak sanitation, and lack of quality control and assurance tools for monitoring water quality. Such situations lead to the generation of water-borne pathogens and the production of infectious diseases that affect a mass number of lives. These water-borne diseases are one of the major contributors to death worldwide. The mortality rate due to water-borne diseases such as typhoid, cholera, polio, and dysentery is recorded to be approximately 5,500 deaths per day worldwide.[1] This rate was found to be very high in rural zones of Asia and Africa where either the essential hygienic tools are predominantly lacking or there is a failure to provide such tools. In such instances, preserving the cleanliness of drinking water resources is difficult. The traditional water quality monitoring analyses require plenty of time, instrument technicians, and state-of-the-art laboratories. Overcoming these constraints is extremely difficult for Third World countries with large populations.[2] Therefore, it is imperative to develop a rapid, inexpensive, eco-friendly, and less laborious method for the point-of-care detection of pathogens that cause water-borne diseases.[3,4] Thus, water-borne pathogens are the major targets of sensing and quantification in various fields such as food safety, public health, and medicine. The presence of *Escherichia coli*, a subgroup of the fecal coliform group, in drinking water usually indicates recent fecal contamination, which may pose an immediate health risk to anyone who consumes such water.[5] Various studies showed that among the class of bacterial pathogens, coliforms are one of the most prominent and dangerous bacterial forms to cause severe health damage to countless lives at an alarming rate.[6−8] Therefore, rapid on-site detection of coliform bacteria in water by a simple and cost-effective method is one of the greatest concerns to save people from water-borne diseases.

Among various sensing mechanisms, electrochemical transduction is an attractive approach to sense and detect biomolecules, diseases, and microbes by employing suitable biorecognition elements to study the electron transfer or

Received: April 25, 2021
Accepted: August 11, 2021
Published: August 30, 2021

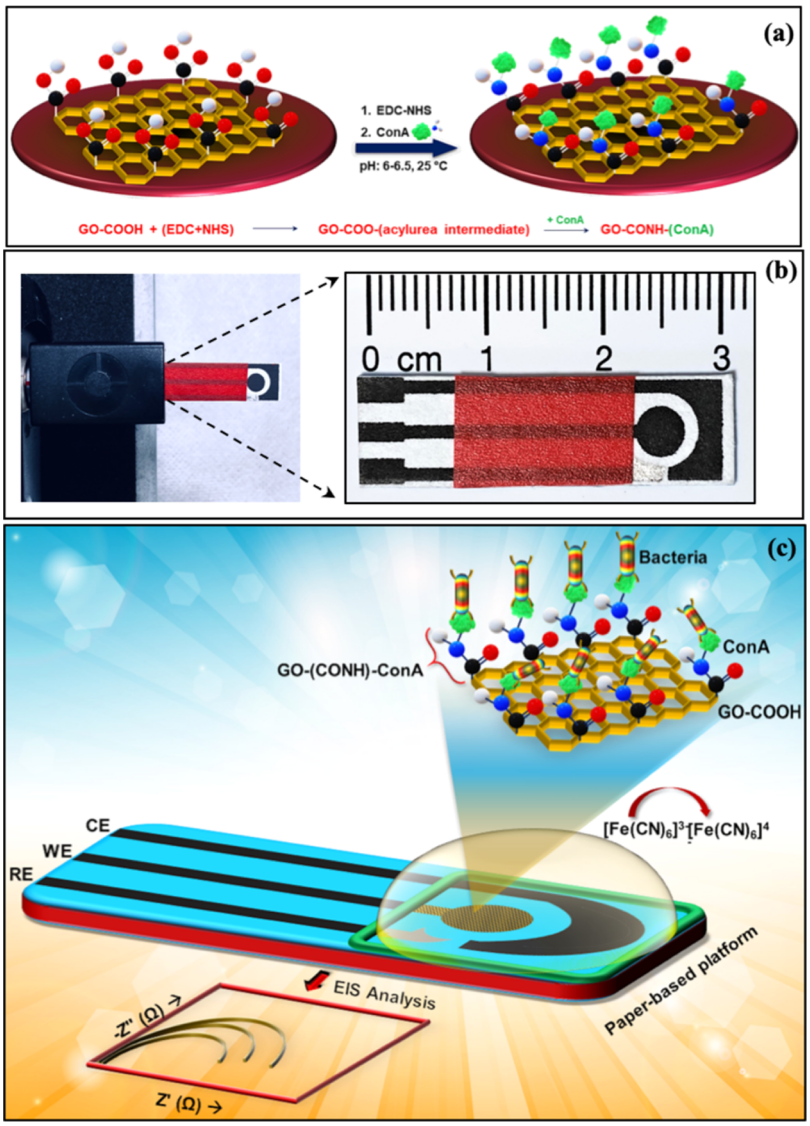

Figure 1. (a) Schematic illustration of the step-by-step fabrication and covalent immobilization of ConA on GO. (b) Fabricated screen-printed paper-based nanobiosensor with the interelectrode distance of 2 mm. (c) Graphical illustration of the detection mechanism of the biosensor by ConA recognition, which leads to further transduction into measurable EIS signals.

diffusion process that occurs at the surface of an electrode.[9−11] It is an excellent method that not only has a low cost but also is easy to operate and durable. Voltammetry, amperometry, and impedimetric biosensors are the key electroanalytical techniques of electrochemical sensing.[12,13] Among them, impedimetric biosensors hold several advantages over other techniques for bioanalysis: (i) they are nondestructive because a small amplitude perturbation from the steady state leaves the electrode surface undamaged after the experiment; (ii) they contribute to a sharp change in the signal when a biorecognition event occurs; and (iii) they are easy to quantify, are efficient for miniaturization, are label-free, and consume less time.[14]

Martinez et al. developed the first paper-based analytical devices (μPADs); since then, paper-based biosensors have emerged as a new class of lab-on-a-chip devices.[15−18] Paper is an excellent material with easy fabrication steps, which allows the synergistic incorporation of highly sensitive methods to facilitate a range of critical functions.[19−23] The surface matrix of paper makes it an extremely active platform for biomolecule immobilization. Also, it possesses notable features such as biocompatibility, porosity, eco-friendliness, and low fabrication cost.[21,24,25] All of these attributes of paper can be deployed to fabricate paper-based biosensors with high precision and accuracy. The paper-based electrochemical biosensing technique was first reported by Dungchai et al. using screen-printed carbon ink to determine the glucose, lactate, and uric acid in biological samples.[26] Other than carbon, there is an increasing number of reports on graphene-based electrodes, due to its large surface area, exceptional electrochemical properties, high mechanical strength, ease of biofunctionalization, and low cost, resulting in graphene-based materials gaining much attention in biosensing applications.[27−29]

The paper-based sensors for detecting bacteria in the food and water samples have been reported earlier;[30,31] these employed a colorimetry-based transduction mechanism,[32−36] where optical signals are detected when the bacteria interact with the biorecognition element present. However, the colorimetric assays, leading to the formation of a chromogenic product during such interactions, show poor sensitivity and

https://doi.org/10.1021/acssensors.1c00851
ACS Sens. 2021, 6, 3214−3223

difficulties in performing quantitative measurements.[37] On the other hand, immunoassay-based detection utilizes antibodies as bioreceptors and usually suffers from low capture efficiency, nonspecific effects, denaturation of the antibody under certain environmental constraints, and expensive and time-consuming analyses, which limit their ultrasensitivity.[38,39]

To encounter these difficulties, we have developed a novel, sensitive, label-free, paper-based impedimetric biosensor for the detection of *E. coli* contamination in water. Specifically, the sensor was fabricated by screen-printing graphene (G) ink on paper, followed by surface modification using graphene oxide (GO). Concanavalin A (ConA), one of the lectins, is used as a biorecognition element due to its specific binding capability toward mono- and oligosaccharides of *E. coli* cells. The electrochemical performance of the fabricated sensor (GGO_ConA) was tested, and its sensitivity toward the detection of bacteria in synthetic wastewater and field water samples collected from a beach was probed. The results were presented and showed a good correlation with the verified data. To prove the selectivity, sensitivity, and superior limit of detection of GGO_ConA over the graphene screen-printed electrode (GSPE), a simultaneous experiment using GSPE was conducted. Compared with the previously reported literature, we have obtained the best limit of detection by far.

RESULTS AND DISCUSSION

Immobilization of Biorecognition Element and Fabrication of the Nanobiosensor. Graphene oxide was synthesized by the Hummers method,[40] graphically shown in Figure S1. The immobilization of the biorecognition element ConA on the screen-printed working electrode (Figure 1a), GGO_ConA, was achieved by EDC-NHS coupling protocols where the carboxyl group of GO covalently bonded with the amine group of ConA by the formation of an amide bond between GO and ConA (Figure 1a).[41,42] Figure 1b presents the paper-based nanobiosensor chip to detect bacterial contamination in water using a cost-effective screen-printing method. The principle and fundamental mechanism behind our paper-based bacterial detection by ConA-modified GO by electrochemical impedance spectroscopy (EIS) are presented graphically in Figure 1c.

X-ray Diffraction (XRD) of Graphite and GO. The XRD patterns of graphite (G) (Figure S2a) exhibited a sharp, high-intensity diffraction peak at 26.4° with an interplanar spacing of 3.38 Å to the (002) plane, whereas in the GO (Figure S2a), the (002) plane was observed at 11° with an interplanar spacing of 8.9 Å: the peak shift is due to the exfoliation of the stacked graphitic layers into few layers of GO. A similar observation has been reported by other researchers previously.[43,44]

UV−vis Spectra of GO. The UV−vis spectra (Figure S2b) of GO sheets revealed an absorption band appearing at 230 nm, which proves the $\pi-\pi^*$ interactions between GO sheets. These interactions are electrostatic in nature and originate from the π plasmon of carbon.[45,46] Further, the nonbonding electrons in the GO layer lead to the $n-\pi^*$ transitions, which is evident from the weak absorption shoulder at around 300 nm. The results were supported by prior works.[47,48]

FTIR Spectroscopy of GO. FTIR spectroscopy (Figure S2c) corroborated the presence of epoxy, hydroxyl, C═O (from carboxyl and carbonyl groups), aliphatic C−H stretching, and C═C stretching.

XPS Measurements. XPS survey spectra revealed the characteristic features of GSPE (screen-printed on paper) and GO (on Si wafer) (Figure S2d). It is observed that carbon and oxygen responsible features were seen in both samples along with the Si-, S-, and F-related peaks, presented in the screen-printing ink.

The C 1s core-level spectra of graphene and GO (Figure 2a,b) were fitted and convoluted into three Gaussian peaks.

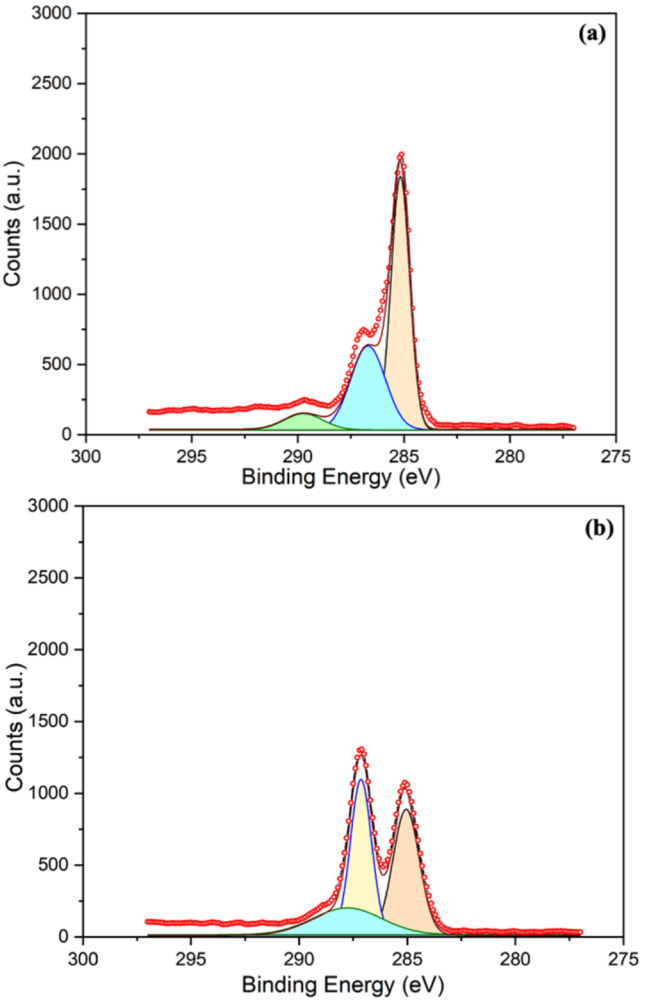

Figure 2. C 1s core-level XPS spectra of (a) GSPE and (b) GO. The open circled curve indicates the raw data and solid lines with the filled area under the curve (deconvoluted components) were obtained by multipeak Gaussian fitting to analyze/quantify the functional groups presented in GSPE and GO.

The C═C peak is mainly attributed to the sp^2-bonded carbon of GSPE and GO with the binding energies (BE) of 284.4 and 284.6 eV, respectively, whereas C−O and −COOH groups in GSPE and GO exhibited peaks obtained in XPS measurements[49] (Table 1).

Morphology of GO by High-Resolution Transmission Electron Microscopy (HRTEM) Image Analysis. The HRTEM images of GO, as shown in Figure 3, show translucence, wrinkles, and folds (Figure 3b) in the GO sheets. This indicates that the synthesized GO is two-dimensional in nature and comprises mono or few layers of the GO. The sheet size was determined and found to be in the range from 1 to 5 μM. The GO layers did not have any

https://doi.org/10.1021/acssensors.1c00851
ACS Sens. 2021, 6, 3214−3223

Table 1. Summary of Fitting Parameters and Relative Percentage of Functional Groups Presented in GSPE and GO

GSPE			GO		
peak	BE (eV)	relative %	peak	BE (eV)	relative %
C=C	284.4	56.7	C=C	284.6	43.3
C−O	287.1	33.5	C−O	287.3	42.7
−COOH	289.5	9.8	−COOH	288.8	14.0

preferential stacking arrangement between neighboring sheets, and this may be due to the fact that the GO was drop-cast on the carbon-coated grid.[41,50]

Electrochemical Studies: Characterization of the Electrodes. The electron-transfer mechanism of the redox probe $[Fe(CN)_6]^{3-/4-}$, occurring at the surface of the GSPE, GGO, and GGO-ConA electrodes, was extensively studied through cyclic voltammetry (CV). The influence of the scan rate on the electrodes (Figures S3a,b and 4a) indicates that the peak current increases with the increasing scan rate. The ratio between the forward and backward peak currents (I_{pa}/I_{pc}) fell in the range of 1.00−1.03. This implies that the electrochemical process follows the quasi-reversible system.[51] The inset of Figure 4a shows the plot of the peak current (I_{pa} and I_{pc}) vs the square root of the scan rate ($\nu^{1/2}$) for the electrodes GSPE, GGO, and GGO_ConA. In the case of GGO and GGO_ConA electrodes, the linear regression coefficients (R^2) for the linear fitting of the points of peak current vs $\nu^{1/2}$ were found to be 0.9992 and 0.9994 for GGO and GGO_ConA electrodes, respectively. The linear nature of the plot indicates that the electrochemical process is diffusion-controlled at the GGO_ConA electrode. This can be quantified by the diffusion coefficient (D), which plays an important role in determining the sensitivity of the electrode.

The diffusion coefficient and the surface concentration of the ferricyanide (for the GSPE and GGO electrodes) were calculated using the Randles−Sevcik equation (eq 1 in the SI)[52,53] and the Brown--Anson model (eq 2 in SI), respectively.[54] The higher diffusion coefficient of ferricyanide for the GGO electrode (1.1×10^{-5} cm^2 s^{-1}) compared to the GSPE (1.3×10^{-6} cm^2 s^{-1}) indicates a faster electron-transfer rate at the GGO electrode compared to that on the GSPE.

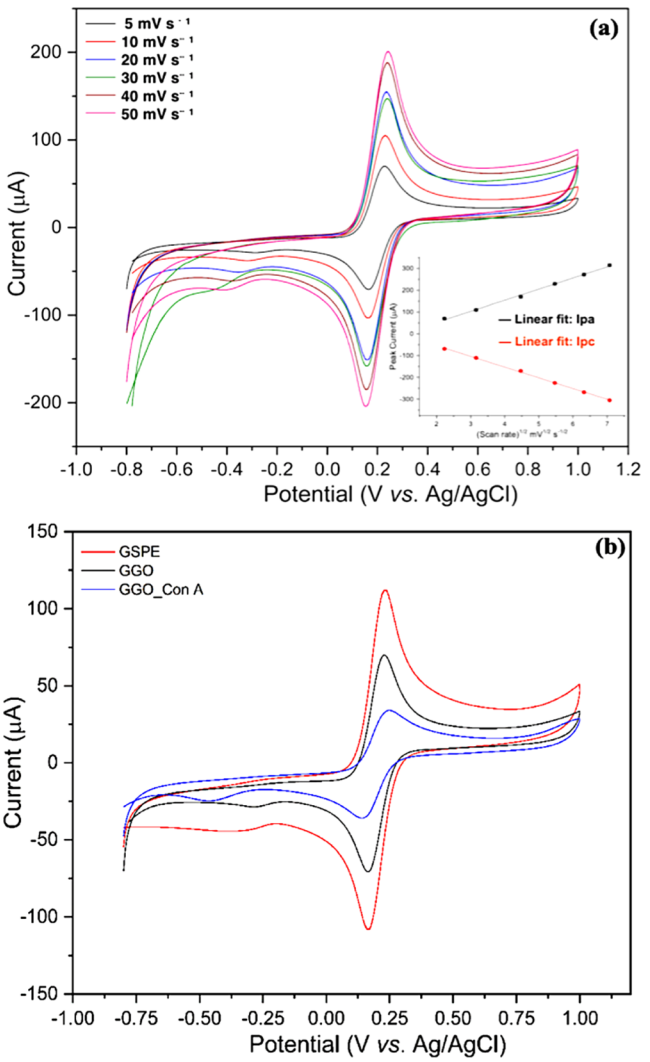

Figure 4. CV curves of the fabricated electrode in the presence of 5 mM $[Fe(CN)_6]^{3-/4-}$ in 0.1 M phosphate-buffered saline (PBS) buffer. (a) GGO_ConA measured at different scan rates; the inset illustrated the linear dependency of peak current vs (scan rate)$^{1/2}$. (b) Comparison of GSPE, GGO and, GGO_ConA electrodes at a scan rate of 5 mV s^{-1}.

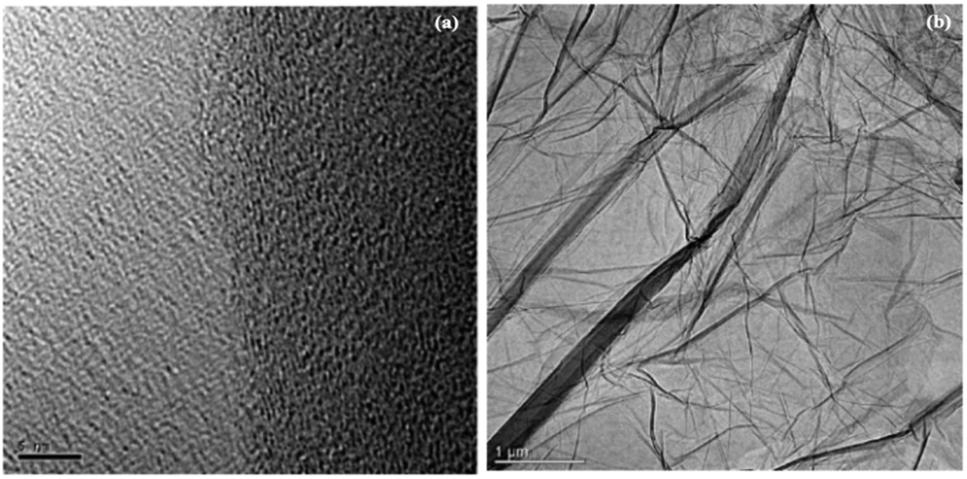

Figure 3. HRTEM Images of GO (drop-cast on carbon grid) sheets. (a) Image at a higher magnification to observe the lattice fringes in GO sheets. (b) Translucent appearance of the GO sheet, indicating the few-layer structure of the synthesized GO.

https://doi.org/10.1021/acssensors.1c00851
ACS Sens. 2021, 6, 3214−3223

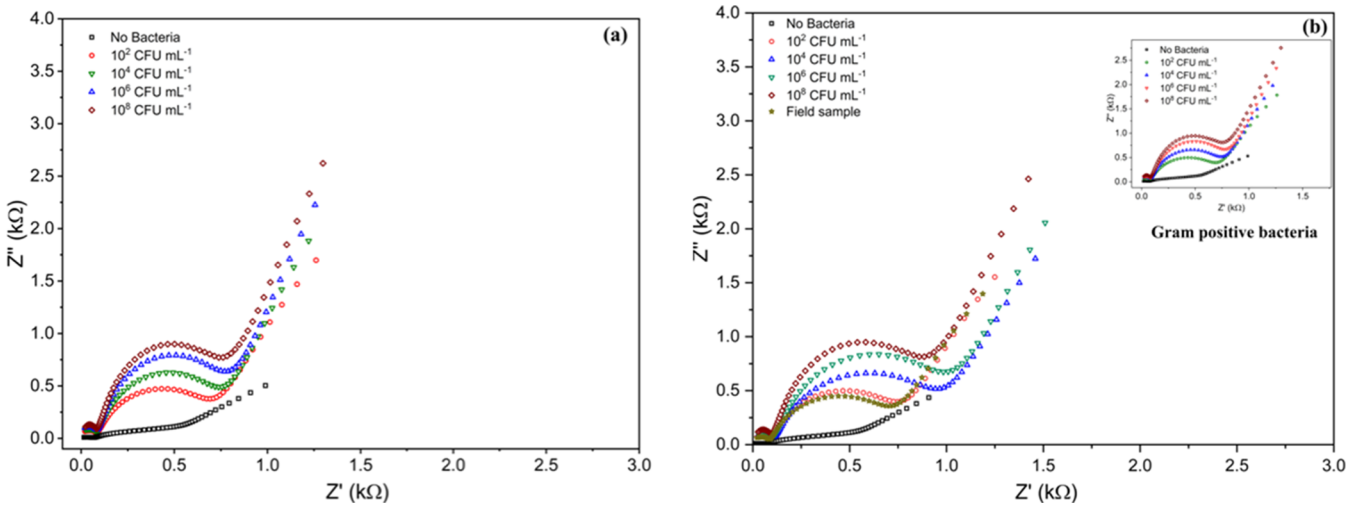

Figure 5. Analytical performance of the paper-based biosensor determined through EIS in the presence of the electrolyte consisting of 5 mM $[Fe(CN)_6]^{3-/4-}$ in 0.1 M of PBS buffer. The EIS measured in the frequency range of 10 Hz to 1 MHz with the applied potential of 0.2 V. In the electrode, ConA immobilized covalently on the surface of GO. (a) Single-sized bacteria (b) different sizes of bacteria, where the inset presents the biosensing behavior of GGO_ConA with Gram-positive bacteria type.

Thus, it is expected that a higher surface concentration of ConA is immobilized on GGO (0.917 $nmol^{-1}$ cm^{-2}) than on the bare GSPE electrode (0.714 $nmol^{-1}$ cm^{-2}), which, in turn, helps capture the bacteria adequately during the sensing analysis. The change in the potential between anodic and cathodic peaks (ΔE_p) with the scan rate is related to the reversible or irreversible behavior of the electrochemical process. For a reversible process, ΔE_p stays constant to the scan rate, and for an irreversible process, the ΔE_p tends to increase with the scan rate. The greater ΔE_p values with the peak broadening were observed for GSPE (Figure S3a). This indicates a slower rate of diffusion, while the mass transfer is predominant over the charge-transfer process at the electrode surface.[55] The standard heterogeneous electron-transfer rate constant, k^o, for two-electrode systems was evaluated using Nicholson's method,[56] given by eqs 3 and 4 in the SI, and found to be 1.01×10^{-3} and 2.04×10^{-3} cm s^{-1} for GSPE and GGO, respectively. As the k^o fulfilled the condition[57] of $0.020 > k^o > 10^{-5}$ cm s^{-1}, the reaction follows the quasi-reversible system mentioned previously (Figures S3 and 4a).

The immobilization of ConA on GGO had been verified through DPV. The electrode immobilized with ConA (GGO_ConA) had an ΔI_p of 46.7 μA while bare GGO had an ΔI_p of 10 μA (Figure S4a). The decrease in the peak current indicates a slower electron transfer, and this may arise due to the large surface area of GO with −COOH. Besides, the electron-transfer kinetics of the GSPE, GGO, and GGO_ConA were studied by Nyquist's plot obtained by the EIS technique (Figure S4b) through the observation of the real part of the impedance in the Nyquist's plot. It is found that the charge-transfer resistance (R_{ct}) of GSPE, GGO, and GGO_ConA electrodes is 0.1 kΩ, 0.8 kΩ, and 1.3 kΩ, respectively. The lower R_{ct} of GSPE and the higher R_{ct} of ConA-immobilized electrode (i.e., GGO_ConA) are as expected due to the ConA immobilization on the surface of GGO.

Analytical Performance of the Biosensing Electrode. The electrodes had been tested for bacterial sensing using the EIS technique where Nyquist's plot provides information about the sensing ability of the concerned system of study (Figures 5 and S5). ConA, physisorbed on the GSPE electrode, shows an irregular trend in the spectrum upon an increase in bacterial concentration (Figure S5).

The electron-transfer resistance was increased in a nonlinear way with poor sensitivity. This may be due to the weak noncovalent binding of ConA through van der Waals forces. Besides, the absence of the −COOH groups in GSPE increases the possibility of nonspecific adsorptions of ConA on the electrode surface, resulting in other side reactions that prohibit the specific interaction of the bacterial cells with the biosensing electrode. Therefore, the ConA-physisorbed GSPE is not a suitable candidate for bacterial sensing. Figure S5b indicates the insensitivity of GGO (without ConA) toward bacterial cells. Thus, it cannot be used for bacterial sensing. This failure arises due to the lack of biorecognition element in the GGO electrode. The GGO_ConA electrode (Figure 5a) showed an exponential increase in the interfacial electron-transfer resistance with the concentration of the bacteria cells. This trend was observed by the increase in the charge-transfer resistance (R_{ct}) presented in Figure 5a. The high sensitivity of the GGO_ConA electrode to the bacterial cells may be due to extensive covalent immobilization of ConA to the large area of GGO surface where plenty of −COOH groups are present to facilitate the binding of ConA. Alava et al.[58] also stated that the self-assembly of lectin ConA through physisorption lacks specificity in detection, but the covalent attachment increases the quality of the biosensor by the increase in lifetime and sensitivity. Also, the EIS measurements were conducted for Gram-positive bacteria and bacteria of different size distribution to test the selectivity of the GGO_ConA electrode (Figure 5b) along with the water sample collected from the beach. Interestingly, the results (Figure 5b and the inset) were corroborated that there was no perturbation in the selectivity and sensitivity of the biosensor as it only relies on the total concentration of bacteria, whose surface is highly specific to the ConA binding. Based on the observation that the Gram-positive bacteria differ from the Gram-negative only by a thin layer of peptidoglycan, which also contains the ConA binding sugars on its surface,[59−61] thus resulting in no significant change in R_{ct} values. In the case of bacteria size influence, the device is designed in such a way that the surface of the ConA

https://doi.org/10.1021/acssensors.1c00851
ACS Sens. 2021, 6, 3214−3223

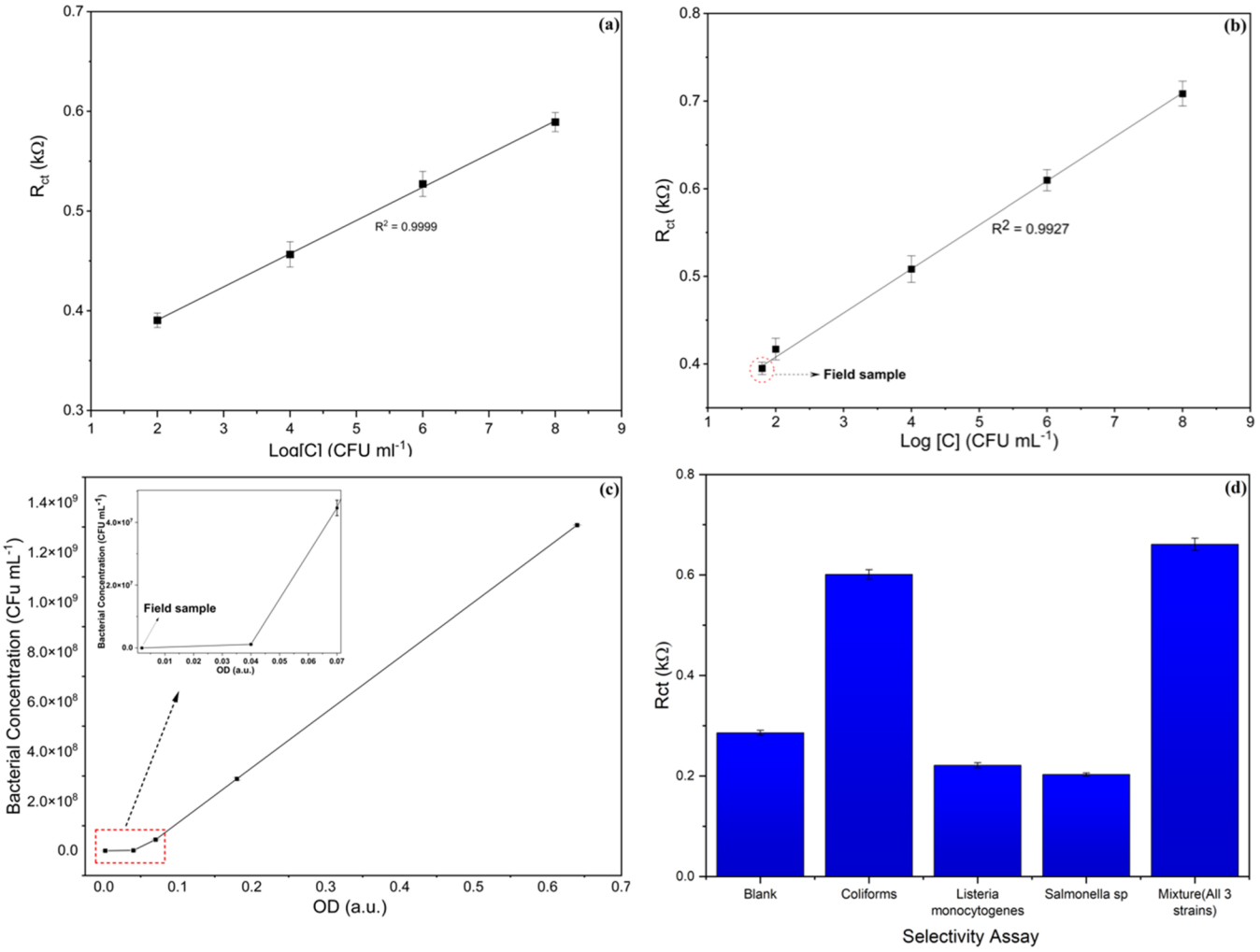

Figure 6. Standardization of the paper-based biosensor. Charge-transfer resistance R_{ct} (obtained from Nyquist's plots) vs log (bacterial concentration) for bacteria of (a) single size and (b) different sizes. (c) OD measurements plotted against the plate count results of the bacteria (the line is drawn to guide the eye), the inset presented is magnified to show the error bar prominent to the reader. (d) Bar graph demonstrated the selectivity and specificity of the biosensor with the least present common strains, as the R_{ct} values derived from the EIS served as a yardstick for validation (Figure S6c).

bound electrode accommodates the specific concentration (CFU mL^{-1}) of bacteria irrespective of their size. The charge-transfer resistance vs the logarithmic concentration of the bacterial cell was plotted to calculate the limit of detection (LOD) and standardize the biosensor (Figure 6a,b). We observed a good linear correlation with LR (linear range) of 10−10^8 CFU mL^{-1} (Table S2), and the impedance of the sensor was saturated above the linear range mentioned. The LOD of the fabricated sensor was found to be 10 CFU mL^{-1} (Table S3) and the limit of quantitation (LOQ) is 23.25 CFU mL^{-1}. The EIS of the real sample falls in the concentration range of 10−10^2 CFU mL^{-1} based on the R_{ct} value. The bacterial concentration of the water collected from the beach was found to be 69.9 CFU mL^{-1}, and the obtained value was further confirmed by the certified data[62] and OD measurements. Meanwhile, a plate count method to quantify the bacterial colonies was conducted simultaneously along with the impedimetric detection (Figure 6c). The obtained results are in good agreement, revealing the reliability of the paper-based biosensor. Also, the reproducibility of the biosensor was determined by measuring the fixed bacterial concentration of 10^4 CFU mL^{-1} in replication of five sets (10, 10^2, 10^4, 10^6, 10^8 CFU mL^{-1}) of experiments per day for 5 days under the same laboratory conditions (Figure S6a). The plot of R_{ct} vs experiment number (Figure S6b) revealed the RSD of R_{ct} values of 2.52%, indicating the excellent reproducibility of the sensor. The same method was adopted for the real sample (four experiments each per day for 4 days) and the RSD was found to be 2.82% (Table S2), which is a widely acceptable limit for an analytical tool to be reproducible and reliable.[63] Furthermore, we have conducted the EIS analysis (Figure S6c) with other strains such as *Salmonella* sp., and Listeria monocytogenes to evaluate the selectivity of the biosensor. It is evident from the R_{ct} values obtained from the EIS analysis that the fabricated sensor possesses good specificity and selectivity over other tested strains, which proves no interference in our specific bacterial detection, as summarized in the bar graph (Figure 6d).

The comparative summary (Table S3) of our work with the previously reported impedimetric bacterial biosensors, indicating our fabricated paper-based biosensor electrode GGO_Co-nA has the lowest LOD with the widest LR in comparison to other electrode systems. This may be due to the large surface area of GO with plenty of −COOH groups, which bind a large

https://doi.org/10.1021/acssensors.1c00851
ACS Sens. 2021, 6, 3214−3223

number of ConA molecules on the active sites of the electrode (GGO), and, in turn, facilitate the bacteria cells to the ConA molecules effectively. Although there have been reports that sulfonated and N-doped graphenes provide exceptional physicochemical properties,[64−67] practical applications of a screen-printed electrochemical biosensor are hampered due to the greater number of processing steps and toxic solvents, which damage the surface of the paper substrate. Thus, our paper-based GGO_ConA nanobiosensing platform could be suitable for scaling up and manufacturing paper-based bacterial sensors.

The results presented here establish the robustness, efficiency, versatility, and sensitivity of the developed paper-based bacterial biosensor. The fabrication method using screen printing is simple to operate, is cost-effective, and avoids the usage of toxic photoresists, and is employed in lithographic techniques. Moreover, hydrophobic paper, used as a substrate, is inexpensive and eco-friendly. Therefore, our platform of bacterial detection with GGO_ConA having extremely low LOD presents great potential in bacterial biosensing applications. Importantly, our proposed device is suitable for point-of-care on-site detection compared to the previously reported paper-based bacterial sensor that needs a beaker-based experimental setup with Ag/AgCl and Pt-wire electrodes[68] and lacks miniaturization.

CONCLUSIONS

Herein, we have demonstrated the complete protocols of the synthesis and fabrication of a point-of-care, label-free, low-cost, eco-friendly, paper-based, screen-printed graphene oxide modified electrochemical impedimetric biosensor utilizing ConA as a biorecognition element to detect bacterial contamination in water. Our well-characterized electrodes showed remarkable improvement in biorecognition element density and electrochemical activity evidenced by cyclic voltammetry, differential pulse voltammetry, and impedance measurements. Furthermore, the large surface area and the chemical activity of graphene oxide on graphene lead to exceptionally specific immobilization of ConA in the bulk amount on the GO surface due to the active −COOH groups participating in site-specific interaction via EDC/NHS coupling at a pH of 4.5−6.0. The biosensor reported here achieved ultrahigh sensitivity for bacterial contamination detection over a wide linear operation range (10^2−10^8 CFU mL^{-1}), as demonstrated by the electrochemical impedance spectra. Moreover, we first reported an ultralow LOD of 0.1 × 10^2 CFU mL^{-1} for a paper-based bacterial biosensor, without any chemical amplification, such as PCR. Our claim was further supported by the simultaneous quantification of the bacteria by the plate counting method, followed by OD measurements in a water sample collected from the local beach. The highly sensitive detection platform, by exploiting paper as a substrate and screen printing as a tool to develop biosensors, engenders a reliable point-of-care alternative for the detection and diagnosis of water-borne pathogens and water-borne diseases present at very low levels. Additionally, our platform greatly enhances the accessibility, robustness, and consistency in detection, which may inspire future label-free nanoarchitectured biosensors.

EXPERIMENTAL SECTION

Materials, Apparatus, and Measurements. Sodium nitrate ($NaNO_3$), hydrogen peroxide (H_2O_2), *N*-ethyl-*N*′-(3-dimethylaminopropyl) carbodiimide hydrochloride (EDC), *N*-hydroxysuccinimide (NHS), potassium hexacyanoferrate(II) trihydrate ($K_4[Fe(CN)_6]\cdot 3H_2O$), potassium hexacyanoferrate(III), ($K_3[Fe(CN)_6]$), ethanolamine ($HOCH_2CH_2NH_2$), hydrochloric acid (37%), and lectin Concanavalin A (ConA) were purchased from Sigma-Aldrich. Graphite was bought from Alfa-Aesar Ltd. Potassium permanganate ($KMnO_4$) was obtained from Showa Chemical Co. Ltd.; sulfuric acid (H_2SO_4) was from Champion Yuan Chemical Co. Ltd.; Gibco (phosphate-buffered saline, PBS) solution (1×) was purchased from Fischer Scientific Ltd. Conductive graphene (G) screen-printing ink was purchased from Haydale Co. Ltd. Hydrophobic, hot-pressed paper (Cheng Tien Intl. Corp., Taiwan) was used as the substrate to fabricate the biosensing electrode. Graphene oxide (GO) was synthesized in our laboratory. Deionized water (Millipore-Q, 18.2 MΩ cm) was used to wash and prepare the aqueous solutions. Screen printing was done using an ATMA AT-25PA flat screen printer by ATMA Champ Ent. Corp., Taiwan. Electrochemical studies were conducted using CHI 700E Potentiostat Instrument guided with a three-electrode system involving Ag/AgCl reference electrode, graphene counter electrode, and various working electrodes, GSPE, GGO, and GGO-ConA. Electrochemical impedance spectroscopy (EIS) measurements were recorded at a potential of 0.2 V in the frequency range of 0.1 Hz to 1 MHz with an amplitude of 0.01 V. All of the electrochemical experiments were conducted in 0.1 M sterile PBS buffer in the presence of the redox probe, $[Fe(CN)_6]^{3-/4-}$. Other apparatus and measurements are given in the SI.

Synthesis of Graphene Oxide. GO was synthesized using modified Hummer's method,[40,69] which is detailed in the SI.

Bacteria Culture. Bacterial cultures of W3110 K-12 in synthetic wastewater were incubated overnight at 37 °C. The synthetic wastewater was prepared according to the previously reported literature and elaborated in the Supporting Information (Methods in the SI).

Fabrication of the GO-Modified Graphene Screen-Printed Electrode (GGO-SPE). Graphene ink was screen-printed on the paper to have graphene SPE (GSPE). Two layers of printing were done to obtain the electrode with low resistance. The measured resistances for single and double layers were found to be 50 and 30 Ω cm^{-2}, respectively. Each layer was cured at room temperature for about 10 min. The GGO electrode was fabricated by drop-casting 20 μL of 1 mg mL^{-1} suspension of GO in DI water onto the GSPE, allowed to dry at room temperature, washed with DI water, and dried in N_2. A microwell reaction chamber of the total volume of 50 μL was created by 3M tape through the punching technique. The constructed device is circular with an electroactive surface area of 0.16 cm^2. The detailed graphical representation is shown in the SI (Figure S1b).

Immobilization of ConA on Electrode Surface. To obtain the GGO-ConA electrode, ConA was immobilized on GGO by the activation of carboxyl groups present in GO using EDC/NHS chemistry. Briefly, EDC (0.5 M) and NHS (0.1 M) solutions were freshly prepared in MES buffer and the GGO was incubated in a 1:1 (v/v) ratio of EDC/NHS by dropping 15 μL of the mixture. Then, the electrode was incubated for about 30 min at room temperature in 10 μL of lectin (ConA) prepared in sodium acetate buffer (0.1 M, 0.2 mg mL^{-1}) of pH 4.5. Afterward, the nonspecifically adsorbed sites were blocked by immersing the electrode in the ethanolamine solution (0.1 M) for 20 min. The electrode was washed with DI water after each step and dried in N_2 gas. The abundance of carboxyl groups on GGO and lectin immobilization on GGO was determined by cyclic voltammetry (CV) and differential pulse voltammetry (DPV) measurements.

Beach Water Sample Preparation. One hundred milliliters of seawater was collected from the designated beach in northern Taiwan (ROC). It was further treated by the membrane filtration method[70] and divided into two parts: one part was used to validate the fabricated nanobiosensor and the other was exploited by the plate count method for OD measurements.

https://doi.org/10.1021/acssensors.1c00851
ACS Sens. 2021, 6, 3214−3223

■ ASSOCIATED CONTENT

Supporting Information

The Supporting Information is available free of charge at https://pubs.acs.org/doi/10.1021/acssensors.1c00851.

Synthesis of graphene oxide, bacteria culture, UV−vis, Fourier transform infrared (FTIR) data, and CV curves for electrodes with description and formulae to determine electrochemical parameters (PDF)

■ AUTHOR INFORMATION

Corresponding Author

Chia-Fu Chou − *Institute of Physics, Academia Sinica, Taipei 11529 Taiwan, ROC; Research Center for Applied Sciences, Academia Sinica, Taipei 11529 Taiwan, ROC;* orcid.org/0000-0003-0070-5556; Phone: +886-2-2789-6761/8907; Email: cfchou@phys.sinica.edu.tw; Fax: +886-2-2651-0704

Authors

Stalin Karuppiah − *Institute of Physics, Academia Sinica, Taipei 11529 Taiwan, ROC; Department of Chemistry, National Taiwan University, Taipei 10617 Taiwan, ROC; Taiwan International Graduate Program (TIGP), Academia Sinica, Taipei 11529 Taiwan, ROC*

Narayan Chandra Mishra − *Indian Institute of Technology, Roorkee 247667 Uttarakhand, India*

Wei-Chen Tsai − *Institute of Physics, Academia Sinica, Taipei 11529 Taiwan, ROC*

Wei-Ssu Liao − *Department of Chemistry, National Taiwan University, Taipei 10617 Taiwan, ROC;* orcid.org/0000-0002-5619-4997

Complete contact information is available at: https://pubs.acs.org/10.1021/acssensors.1c00851

Author Contributions

S.K. conceived the study and wrote the manuscript. W.C.T. helped the bacteria culture experiments. C.-F.C. supervised the project. S.K. and C.-F.C. co-revised the manuscript. All other authors contributed to guiding the work.

Notes

The authors declare no competing financial interest.

■ ACKNOWLEDGMENTS

The authors acknowledge the technical assistance from the Central Instrumentation Facility (CIF), National Taiwan University for conducting HRTEM measurements: H.-B. Chen for XPS measurements; I.-H. Chen for Nanocore Facilities, Academia Sinica (AS); B. Navaneethan and D.-K. Yang for valuable discussions about bacterial studies; and R. Vikram, Institute of Biomedical Sciences, AS, for assistance in bacterial strain collection. S.K. is grateful to the Ministry of Science and Technology (MOST), Taiwan, for travel grant support. This work is supported by Academia Sinica (grant #AS-IA-109-M04) and Ministry of Science and Technology (MOST, Taiwan, ROC, grants #107-2923-M-001-011-MY3, 108-2112-M-001-023-MY3, 108-2119-M-001-017, 109-2124-M-001-003, and 110-2124-M-001-003).

■ REFERENCES

(1) World Health Organization. *Guidelines for Drinking-Water Quality: Fourth Edition Incorporating the First Addendum*, 978-92-4-154995-0, 2017; p 631.

(2) Gorman, M. E.; Wardak, A.; Fauss, E.; Swami, N. A Framework for Using Nanotechnology To Improve Water Quality. In *Nanotechnology Applications for Clean Water*; Savage, N.; Mamadou, D.; Duncan, J.; Street, A.; Sustich, R., Eds.; William Andrew Publishing, 2009; pp 491−507.

(3) Sharma, S.; Zapatero-Rodríguez, J.; Estrela, P.; O'Kennedy, R. Point-of-care diagnostics in low resource settings: present status and future role of microfluidics. *Biosens. Bioelectron.* **2015**, *5*, 577−601.

(4) Lagarde, F.; Jaffrezic-Renault, N. Cell-based electrochemical biosensors for water quality assessment. *Anal. Bioanal. Chem.* **2011**, *400*, 947−964.

(5) *Departmenet of Health: Coliform Bacteria and Drinking Water*; Office of Drinking Water: Washington, 2016.

(6) Sales-Ortells, H.; Agostini, G.; Medema, G. Quantification of waterborne pathogens and associated health risks in urban water. *Environ. Sci. Technol.* **2015**, *49*, 6943−6952.

(7) Edberg, S. C.; Rice, E. W.; Karlin, R. J.; Allen, M. J. Escherichia coli: the best biological drinking water indicator for public health protection. *J. Appl. Microbiol.* **2000**, *88*, 106S−116S.

(8) Gutiérrez-del-Río, I.; Marin, L.; Fernandez, J.; Alvarez San Millan, M.; Ferrero, F. J.; Valledor, M.; Campo, J. C.; Cobian, N.; Mendez, I.; Lombo, F. Development of a biosensor protein bullet as a fluorescent method for fast detection of Escherichia coli in drinking water. *PLoS One* **2018**, *13*, No. e0184277.

(9) Morales, M. A.; Halpern, J. M. Guide to Selecting a Biorecognition Element for Biosensors. *Bioconjug. Chem.* **2018**, *29*, 3231−3239.

(10) Baryeh, K.; Takalkar, S.; Lund, M.; Liu, G., Introduction to medical biosensors for point of care applications. In *Medical Biosensors for Point of Care (POC) Applications*, Narayan, R. J., Ed.; Woodhead Publishing, 2017; pp 3−25.

(11) Wu, X.; Hou, L.; Lin, X.; Xie, Z., Application of Novel Nanomaterials for Chemo- and Biosensing of Algal Toxins in Shellfish and Water. In *Novel Nanomaterials for Biomedical, Environmental and Energy Applications*, Wang, X.; Chen, X., Eds.; Elsevier, 2019; pp 353−414.

(12) Daniels, J. S.; Pourmand, N. Label-Free Impedance Biosensors: Opportunities and Challenges. *Electroanalysis* **2007**, *19*, 1239−1257.

(13) Ahmed, A.; Rushworth, J. V.; Hirst, N. A.; Millner, P. A. Biosensors for whole-cell bacterial detection. *Clin. Microbiol. Rev.* **2014**, *27*, 631−646.

(14) Bahadır, E. B.; Sezginturk, M. K. A review on impedimetric biosensors. *Artif. Cells, Nanomed., Biotechnol.* **2016**, *44*, 248−262.

(15) Cate, D. M.; Adkins, J. A.; Mettakoonpitak, J.; Henry, C. S. Recent developments in paper-based microfluidic devices. *Anal. Chem.* **2015**, *87*, 19−41.

(16) Martinez, A. W.; Phillips, S. T.; Whitesides, G. M.; Carrilho, E. Diagnostics for the developing world: microfluidic paper-based analytical devices. *Anal. Chem.* **2010**, *82*, 3−10.

(17) Liu, P.; Li, B.; Fu, L.; Huang, Y.; Man, M.; Qi, J.; Sun, X.; Kang, Q.; Shen, D.; Chen, L. Hybrid Three Dimensionally Printed Paper-Based Microfluidic Platform for Investigating a Cell's Apoptosis and Intracellular Cross-Talk. *ACS Sens.* **2020**, *5*, 464−473.

(18) Ding, J.; Li, B.; Chen, L.; Qin, W. A Three-Dimensional Origami Paper-Based Device for Potentiometric Biosensing. *Angew. Chem., Int. Ed.* **2016**, *55*, 13033−13037.

(19) Wang, S.; Ge, L.; Song, X.; Yan, M.; Ge, S.; Yu, J.; Zeng, F. Simple and covalent fabrication of a paper device and its application in sensitive chemiluminescence immunoassay. *Analyst* **2012**, *137*, 3821−3827.

(20) Cheng, C. M.; Martinez, A. W.; Gong, J.; Mace, C. R.; Phillips, S. T.; Carrilho, E.; Mirica, K. A.; Whitesides, G. M. Paper-based ELISA. *Angew. Chem., Int. Ed.* **2010**, *49*, 4771−4774.

(21) Sakata, T.; Hagio, M.; Saito, A.; Mori, Y.; Nakao, M.; Nishi, K. Biocompatible and flexible paper-based metal electrode for potentiometric wearable wireless biosensing. *Sci. Technol. Adv. Mater.* **2020**, *21*, 379−387.

(22) Liana, D. D.; Raguse, B.; Gooding, J. J.; Chow, E. Recent Advances in Paper-Based Sensors. *Sensors* **2012**, *12*, 11505−11526.

(23) Han, J.; Qi, A.; Zhou, J.; Wang, G.; Li, B.; Chen, L. Simple Way To Fabricate Novel Paper-Based Valves Using Plastic Comb Binding Spines. *ACS Sens.* **2018**, *3*, 1789−1794.
(24) Zhao, M.; Li, H.; Liu, W.; Guo, Y.; Chu, W. Plasma treatment of paper for protein immobilization on paper-based chemiluminescence immunodevice. *Biosens. Bioelectron.* **2016**, *79*, 581−588.
(25) Medawar, V.; Messina, G. A.; Fernández-Baldo, M.; Raba, J.; Pereira, S. V. Fluorescent immunosensor using AP-SNs and QDs for quantitation of IgG anti- Toxocara canis. *Microchem. J.* **2017**, *130*, 436−441.
(26) Dungchai, W.; Chailapakul, O.; Henry, C. S. Electrochemical detection for paper-based microfluidics. *Anal. Chem.* **2009**, *81*, 5821−5826.
(27) Sanghavi, B. J.; Varhue, W.; Rohani, A.; Liao, K. T.; Bazydlo, L. A.; Chou, C. F.; Swami, N. S. Ultrafast immunoassays by coupling dielectrophoretic biomarker enrichment in nanoslit channel with electrochemical detection on graphene. *Lab Chip* **2015**, *15*, 4563−4570.
(28) Kim, J.; Park, S. J.; Min, D. H. Emerging Approaches for Graphene Oxide Biosensor. *Anal. Chem.* **2017**, *89*, 232−248.
(29) Fan, Y.; Shi, S.; Ma, J.; Guo, Y. A paper-based electrochemical immunosensor with reduced graphene oxide/thionine/gold nanoparticles nanocomposites modification for the detection of cancer antigen 125. *Biosens. Bioelectron.* **2019**, *135*, 1−7.
(30) Jokerst, J. C.; Adkins, J. A.; Bisha, B.; Mentele, M. M.; Goodridge, L. D.; Henry, C. S. Development of a paper-based analytical device for colorimetric detection of select foodborne pathogens. *Anal. Chem.* **2012**, *84*, 2900−2907.
(31) Adkins, J. A.; Boehle, K.; Friend, C.; Chamberlain, B.; Bisha, B.; Henry, C. S. Colorimetric and Electrochemical Bacteria Detection Using Printed Paper- and Transparency-Based Analytic Devices. *Anal. Chem.* **2017**, *89*, 3613−3621.
(32) Li, C. Z.; Vandenberg, K.; Prabhulkar, S.; Zhu, X.; Schneper, L.; Methee, K.; Rosser, C. J.; Almeide, E. Paper based point-of-care testing disc for multiplex whole cell bacteria analysis. *Biosens. Bioelectron.* **2011**, *26*, 4342−4348.
(33) Hossain, S. M.; Ozimok, C.; Sicard, C.; Aguirre, S. D.; Ali, M. M.; Li, Y.; Brennan, J. D. Multiplexed paper test strip for quantitative bacterial detection. *Anal. Bioanal. Chem.* **2012**, *403*, 1567−1576.
(34) Struss, A.; Pasini, P.; Ensor, C. M.; Raut, N.; Daunert, S. Paper strip whole cell biosensors: a portable test for the semiquantitative detection of bacterial quorum signaling molecules. *Anal. Chem* **2010**, *82*, 4457−4463.
(35) Morales-Narváez, E.; Golmohammadi, H.; Naghdi, T.; Yousefi, H.; Kostiv, U.; Horak, D.; Pourreza, N.; Merkoci, A. Nanopaper as an Optical Sensing Platform. *ACS Nano* **2015**, *9*, 7296−7305.
(36) Li, B.; Zhang, Z.; Qi, J.; Zhou, N.; Qin, S.; Choo, J.; Chen, L. Quantum Dot-Based Molecularly Imprinted Polymers on Three-Dimensional Origami Paper Microfluidic Chip for Fluorescence Detection of Phycocyanin. *ACS Sens.* **2017**, *2*, 243−250.
(37) Orenga, S.; James, A. L.; Manafi, M.; Perry, J. D.; Pincus, D. H. Enzymatic substrates in microbiology. *J. Microbiol. Methods* **2009**, *79*, 139−155.
(38) Tlili, C.; Sokullu, E.; Safavieh, M.; Tolba, M.; Ahmed, M. U.; Zourob, M. Bacteria screening, viability, and confirmation assays using bacteriophage-impedimetric/loop-mediated isothermal amplification dual-response biosensors. *Anal. Chem.* **2013**, *85*, 4893−4901.
(39) Wu, Y.; Tilley, R. D.; Gooding, J. J. Challenges and Solutions in Developing Ultrasensitive Biosensors. *J. Am. Chem. Soc.* **2019**, *141*, 1162−1170.
(40) Hummers, W. S.; Offeman, R. E. Preparation of Graphitic Oxide. *J. Am. Chem. Soc.* **1958**, *80*, 1339.
(41) Verma, S.; Singh, A.; Shukla, A.; Kaswan, J.; Arora, K.; Ramirez-Vick, J.; Singh, P.; Singh, S. P. Anti-IL8/AuNPs-rGO/ITO as an Immunosensing Platform for Noninvasive Electrochemical Detection of Oral Cancer. *Appl. Mater. Interfaces* **2017**, *9*, 27462−27474.
(42) Hernández, R.; Vallés, C.; Benito, A. M.; Maser, W. K.; Rius, F. X.; Riu, J. J. B. Graphene-based potentiometric biosensor for the immediate detection of living bacteria. *Biosens. Bioelectron.* **2014**, *54*, 553−557.
(43) Moon, I. K.; Lee, J.; Ruoff, R. S.; Lee, H. Reduced graphene oxide by chemical graphitization. *Nat. Commun.* **2010**, *1*, No. 73.
(44) Marcano, D. C.; Kosynkin, D. V.; Berlin, J. M.; Sinitskii, A.; Sun, Z.; Slesarev, A.; Alemany, L. B.; Lu, W.; Tour, J. M. Improved synthesis of graphene oxide. *ACS Nano* **2010**, *4*, 4806−4814.
(45) Reed, B. W.; Sarikaya, M. Electronic properties of carbon nanotubes by transmission electron energy-loss spectroscopy. *Phys. Rev. B* **2001**, *64*, No. 195404.
(46) Attal, S.; Thiruvengadathan, R.; Regev, O. Determination of the concentration of single-walled carbon nanotubes in aqueous dispersions using UV−visible absorption spectroscopy. *Anal. Chem.* **2006**, *78*, 8098−8104.
(47) Zhang, J.; Yang, H.; Shen, G.; Cheng, P.; Zhang, J.; Guo, S. Reduction of graphene oxide via L-ascorbic acid. *Chem. Commun.* **2010**, *46*, 1112−1114.
(48) Li, J.; Liu, C.-y.; Liu, Y. Au/graphene hydrogel: synthesis, characterization and its use for catalytic reduction of 4-nitrophenol. *J. Mater. Chem.* **2012**, *22*, 8426−8430.
(49) Mattevi, C.; Eda, G.; Agnoli, S.; Miller, S.; Mkhoyan, K. A.; Celik, O.; Mastrogiovanni, D.; Granozzi, G.; Garfunkel, E.; Chhowalla, M. Evolution of Electrical, Chemical, and Structural Properties of Transparent and Conducting Chemically Derived Graphene Thin Films. *Adv. Funct. Mater.* **2009**, *19*, 2577−2583.
(50) Wilson, N. R.; Pandey, P. A.; Beanland, R.; Young, R. J.; Kinloch, I. A.; Gong, L.; Liu, Z.; Suenaga, K.; Rourke, J. P.; York, S. J.; Sloan, J. Graphene oxide: structural analysis and application as a highly transparent support for electron microscopy. *ACS Nano* **2009**, *3*, 2547−2556.
(51) Wang, J. *Analytical Electrochemistry*, 3rd ed.; Wiley-VCH: USA, 2006; Vol. *272*.
(52) Bard, A. J.; Larry, R. F. *Electrochemical Methods: Fundamentals and Applications*; Wiley: New York, 2000; p864.
(53) Chang, H.-C.; Wu, C.-C.; Ding, S.-J.; Lin, I. S.; Sun, I. W. Measurement of diffusion and partition coefficients of ferrocyanide in protein-immobilized membranes. *Anal. Chim. Acta* **2005**, *532*, 209−214.
(54) Brown, A. P.; Anson, F. C. Cyclic and differential pulse voltammetric behavior of reactants confined to the electrode surface. *Anal. Chem.* **1977**, *49*, 1589−1595.
(55) Banks, C. E.; Brownson, D. A. C. *The Handbook of Graphene Electrochemistry*; Springer-Verlag Ltd., 2014.
(56) Nicholson, R. S. Theory and Application of Cyclic Voltammetry for Measurement of Electrode Reaction Kinetics. *Anal. Chem.* **1965**, *37*, 1351−1355.
(57) Gosser, D. K. *Cyclic Voltammetry: Simulation and Analysis of Reaction Mechanisms*; Wiley-VCH: New York, 1993.
(58) Alava, T.; Mann, J. A.; Theodore, C.; Benitez, J. J.; Dichtel, W. R.; Parpia, J. M.; Craighead, H. G. Control of the graphene-protein interface is required to preserve adsorbed protein function. *Anal. Chem.* **2013**, *85*, 2754−2759.
(59) Lehotzky, R. E.; Partch, C. L.; Mukherjee, S.; Cash, H. L.; Goldman, W. E.; Gardner, K. H.; Hooper, L. V. Molecular basis for peptidoglycan recognition by a bactericidal lectin. *Proc. Natl. Acad. Sci. U.S.A.* **2010**, *107*, 7722−7727.
(60) Gottenbos, B.; Grijpma, D. W.; van der Mei, H. C.; Feijen, J.; Busscher, H. J. Antimicrobial effects of positively charged surfaces on adhering Gram-positive and Gram-negative bacteria. *J. Antimicrob. Chemother.* **2001**, *48*, 7−13.
(61) Kumar, S.; Ingle, H.; Prasad, D. V.; Kumar, H. Recognition of bacterial infection by innate immune sensors. *Crit. Rev. Microbiol.* **2013**, *39*, 229−246.
(62) Environmental Protection Agency, T., Taiwan Beach water quality monitoring 2018. Management. Department and Environmental Impact and Assessment.
(63) AOAC. *AOAC Peer-verified Methods Program: Manual on Policies and Procedures*; Association of Official Analytical Chemists, 1993.

https://doi.org/10.1021/acssensors.1c00851
ACS Sens. 2021, 6, 3214−3223

(64) Yu, W.; Sisi, L.; Haiyan, Y.; Jie, L. Progress in the functional modification of graphene/graphene oxide: a review. *RSC Adv.* **2020**, *10*, 15328−15345.
(65) Mohammadi, O.; Golestanzadeh, M.; Abdouss, M. Recent advances in organic reactions catalyzed by graphene oxide and sulfonated graphene as heterogeneous nanocatalysts: a review. *New. J. Chem.* **2017**, *41*, 11471−11497.
(66) Wang, Y.; Shao, Y.; Matson, D. W.; Li, J.; Lin, Y. Nitrogen-Doped Graphene and Its Application in Electrochemical Biosensing. *ACS Nano* **2010**, *4*, 1790−1798.
(67) Kaushal, S.; Kaur, M.; Kaur, N.; Kumari, V.; Singh, P. P. Heteroatom-doped graphene as sensing materials: a mini review. *RSC Adv.* **2020**, *10*, 28608−28629.
(68) Rengaraj, S.; Cruz-Izquierdo, Á.; Scott, J. L.; Di Lorenzo, M. Impedimetric paper-based biosensor for the detection of bacterial contamination in water. *Sens. Actuators, B* **2018**, *265*, 50−58.
(69) Cote, L. J.; Kim, F.; Huang, J. Langmuir-Blodgett assembly of graphite oxide single layers. *J. Am. Chem. Soc.* **2009**, *131*, 1043−1049.
(70) Bartram, J.; Ballance, R.; world health organization; United Nations Environment Programme *Water Quality Monitoring: A Practical Guide to the Design and Implementation of Freshwater Quality Studies and Monitoring Programs*; E & FN Spon: London, 1996; p 383.

https://doi.org/10.1021/acssensors.1c00851
ACS Sens. 2021, 6, 3214−3223